AIP | Journal of Applied Physics

Intensity distributions of enhanced H emission from laser-induced low-pressure He plasma and a suggested He-assisted excitation mechanism

Zener Sukra Lie, Marincan Pardede, Rinda Hedwig, Maria Margaretha Suliyanti, Eden Steven, Maliki, Koo Hendrik Kurniawan, Muliadi Ramli, Syahrun Nur Abdulmadjid, Nasrullah Idris, Kurnia Lahna, Kiichiro Kagawa, and May On Tjia

Citation: Journal of Applied Physics **106**, 043303 (2009); doi: 10.1063/1.3195087

View online: http://dx.doi.org/10.1063/1.3195087

View Table of Contents: http://scitation.aip.org/content/aip/journal/jap/106/4?ver=pdfcov

Published by the AIP Publishing

Intensity distributions of enhanced H emission from laser-induced low-pressure He plasma and a suggested He-assisted excitation mechanism

Zener Sukra Lie,[1] Marincan Pardede,[1] Rinda Hedwig,[1] Maria Margaretha Suliyanti,[1] Eden Steven,[1] Maliki,[1] Koo Hendrik Kurniawan,[1,a)] Muliadi Ramli,[2] Syahrun Nur Abdulmadjid,[3] Nasrullah Idris,[3] Kurnia Lahna,[3] Kiichiro Kagawa,[4] and May On Tjia[5]

[1]*Research Center of Maju Makmur Mandiri Foundation, 40 Srengseng Raya, Kembangan, Jakarta Barat 11630, Indonesia*
[2]*Department of Chemistry, Faculty of Mathematics and Natural Sciences, Syiah Kuala University, Darussalam, Banda Aceh, Nanggroe Aceh Darussalam 23111, Indonesia*
[3]*Department of Physics, Faculty of Mathematics and Natural Sciences, Syiah Kuala University, Darussalam, Banda Aceh, Nanggroe Aceh Darussalam 23111, Indonesia*
[4]*Department of Physics, Faculty of Education and Regional Studies, Fukui University, 9-1 bunkyo 3-chome, Fukui 910-8507, Japan*
[5]*Physics of Magnetism and Photonics Group, Faculty of Mathematics and Natural Sciences, Bandung Institute of Technology, 10 Ganesha, Bandung 40132, Indonesia*

(Received 17 March 2009; accepted 9 July 2009; published online 18 August 2009)

An experimental study was conducted on the spatial distributions of hydrogen emission intensities from low-pressure plasmas generated by laser ablation of zircaloy-4 and black stone targets in nitrogen and helium ambient gases. In addition to confirming the previously observed intensity enhancement effect in ambient helium gas, the hydrogen and helium emission intensities measured along the plasma expansion direction revealed remarkable extended spatial distributions featuring unexpected maxima near the far end of the plasma where the available shock-wave generated thermal excitation energy should have been significantly reduced. This "anomalous" feature necessarily implied the presence of an additional excitation process beside the well known shock-wave excitation process which is responsible for the plasma emission of heavy atoms in low-pressure ambient gas. Further analysis of the data led to a suggested physical mechanism explaining the possible contribution of a helium metastable excited state to the unusual phenomenon observed in this experiment. © *2009 American Institute of Physics*. [DOI: 10.1063/1.3195087]

I. INTRODUCTION

It is well known that hydrogen emission from laser-induced plasma in atmospheric-pressure ambient air invariably suffers from the unfavorable effects of line broadening and intensity diminution.[1] This problem has long been a blemish for the otherwise highly successful and widely adopted technique of laser-induced breakdown spectroscopy (LIBS).[2,3] Since hydrogen analysis has important applications in scientific research as well as in industrial investigation, overcoming this long standing problem will allow the LIBS method to better serve the scientific and industrial needs, given the advantage of its already highly developed technique.

In a series of experimental studies on the emission spectra of halogen gases and sulfur in laser-induced plasma at atmospheric pressure, the uses of ambient helium gas were invariably shown to result in emission intensity enhancement[4–6] and reduction in Stark broadening effect.[7] Although the possible contribution of the He metastable excited state was suggested in works dating back to early 1990s,[8–10] no conclusive data and detailed discussion have so far been reported on the possible physical origin of those interesting and important effects. These favorable effects of ambient helium gas was further confirmed and substantiated by the reported observation on the emission of hydrogen impurity in zircaloy-4 samples detected from its low-pressure[11] as well as atmospheric helium plasma.[12] Based on the analysis of the spatially integrated time-resolved spectral data obtained in a subsequent experiment for hydrogen and helium emission intensities,[13] the favorable effects of ambient helium gas were shown to be closely related to the possible role of a helium metastable excited state in the delayed excitation of hydrogen atoms in the plasma, and thereby circumventing the previously reported time mismatch effect suffered by very light atoms such as hydrogen.[14] This effect was described as a reduced effectiveness of the shock-wave excitation mechanism due to the premature passage of the fast moving small H atoms prior to the shock-wave formation by the much heavier and relatively slow moving major host atoms. Nevertheless, additional experimental data are required for further clarification on the role of He metastable excited state.

It is important to stress that previous studies on the possible contribution of He metastable excited state to the intensity enhancement effect were performed based on the spatially integrated time-dependent emission data. It is expected

a)Author to whom correspondence should be addressed. Electronic mail: kurnia18@cbn.net.id.

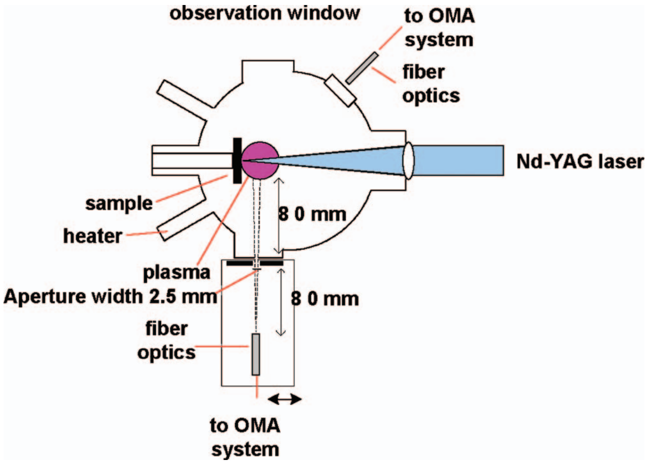

FIG. 1. (Color) Description of experimental setup showing its main features.

that the more detailed information provided by the spatial intensity distribution will shed some light on the above-mentioned issue. Such data are, however, difficult to obtain from the atmospheric-pressure plasma due to its tiny size. The opportunity for such a measurement is indeed provided only by the case of low-pressure ambient gas, where a plasma of much larger size is usually produced. This experiment is specifically designed to take advantage of this feature for the above-mentioned study. It will be shown that the resulted data and their analysis do reveal further support for the suggested additional excitation process in the presence of He ambient gas.

II. EXPERIMENTAL PROCEDURE

The basic experimental setup used in this study is shown in Fig. 1. The cylindrical chamber was equipped with several through ports to allow for temperature and pressure controls as well as the performance of a number of complimentary detections. The laser employed [Nd doped yttrium aluminum garnet (Nd-YAG), Quanta Ray Lab Series, 1064 nm, 8 ns, maximum energy of 450 mJ] was operated in the Q-switched mode at 10 Hz repetition rate with the laser output energy fixed at 68 mJ by means of a set of filters. The laser beam was defocused to a point at 20 mm in front of the sample surface by a movable lens of 250 mm focal length.

One of the targets employed in this experiment was a sample of black stone which was chosen for the simple reason that it produced well known and intense Ca emission lines within the spectral window of present experiment. One of those emission lines (Ca I 649.3 nm) was later used for normalizing the H and He emission intensities. Another sample chosen for this experiment was a zircaloy plate with 8000 ppm of hydrogen which was already used in a previous study of spatially integrated hydrogen emission intensity.[12] All the samples measure 10×10 mm^2 in cross sectional area and 1 mm in thickness. After placing the sample in the chamber, the chamber was evacuated using a vacuum pump to a pressure of 0.001 Torr. High purity helium gas (Air Liquid, 5N) or high purity nitrogen gas (Air Liquid, 5N) was then introduced into the chamber until the desired pressure was reached. This gas pressure was subsequently kept constant during the ensuing experiment.

The plasma emission was detected by means of an optical multichannel analyzer (OMA) system which receives its input from an optical fiber with the fiber entrance end attached to the chamber at a position about 100 mm from the plasma center in the direction making an angle of 45° with the laser beam, as shown in Fig. 1. At this position, the fiber was expected to collect the emitted light entering within 27° of solid angle. Two OMA systems of different resolutions were used in this experiment. The OMA system with high resolutions of 0.009 nm at 500 nm consisted of an OMA (Andor I^*Star intensified charge coupled device (CCD) 1024×256 pixels) and a high resolution spectrograph (McPherson model 2061 with 1000 mm focal length $f/8.6$ Czerny–Turner configuration) with a detector having a spectral width of 20 nm at 500 nm. For the low resolution measurement, another OMA (Princeton Instrument IRY-700) was employed in combination with a spectrograph having a focal length of 150 mm (Acton Research). This system has a spectral resolution of 0.4 nm at 500 nm. The detector used in this system has a spectral window of 80 nm at 500 nm. Both OMA systems were operated at the same gate delay and gate width of 2 μs and 50 μs, respectively. It was observed in the preliminary experiment that a crater was invariably created on the black stone surface upon repeated irradiation, while the zircaloy sample was free from that effect. This different phenomena apparently have their origins in the different melting points of the two samples since the black stone is mainly composed of Ca while the zircaloy sample is mainly composed of the Zr which has considerably higher melting point. Therefore, only the black stone sample was rotated at 2 rpm during the successive laser irradiation in the following experiment. The accumulation of 100 detected spectra at each experimental setting was monitored on a screen, recorded, and averaged to yield the data presented in this report.

For the measurement of spatial distributions of the plasma emission intensities, the lens imaging system employed previously for spatially integrated information[12,13] was replaced by a simple local light collecting gadget inserted in front of the detecting system. As shown in Fig. 1, an aperture of 2.5 mm slit width and 15 mm slit height was attached to one of the entry ports and combined in a movable housing with a fiber having its entrance end positioned behind the aperture at a distance of 160 mm from the plasma axis. Under this condition, the plasma emission area of about 3 mm wide can be fully covered by the detection system. By moving the housing stepwise (at a step of 5 mm) along the plasma axis, the emission intensity can be detected slicewise as a function of the detection position with respect to the target surface. The result will be a longitudinal spatial distribution profile of the emission intensity along the direction of plasma expansion. We shall henceforth refer to this simple measurement procedure as a "plasma slicing technique."

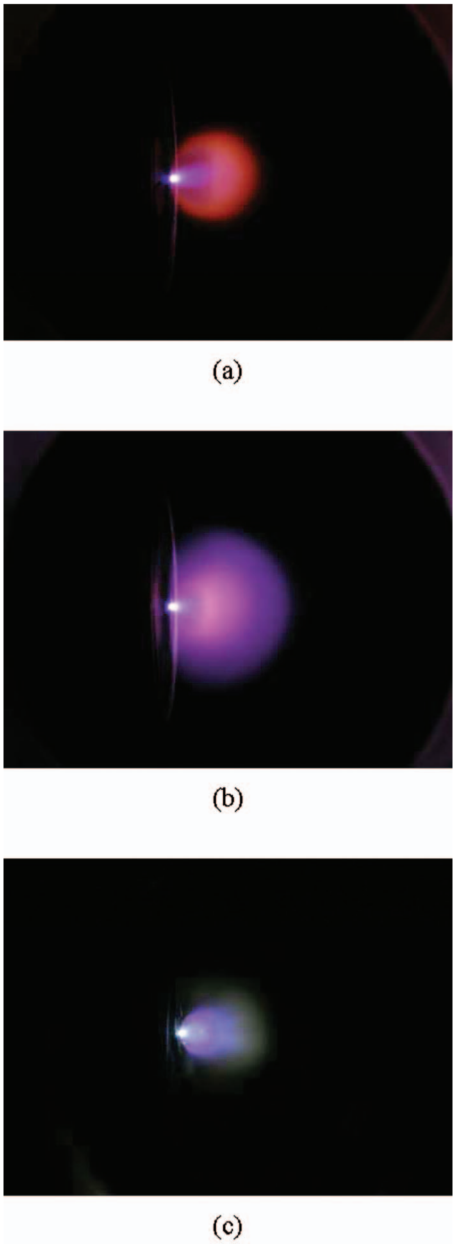

FIG. 2. (Color) Photograph of the plasmas generated by Nd-YAG laser irradiation on (a) black stone sample in 2 Torr ambient nitrogen gas, (b) black stone sample in 20 Torr ambient helium gas, and (c) zircaloy sample in 20 Torr ambient helium gas.

III. EXPERIMENTAL RESULTS AND DISCUSSION

In relation to the spatial intensity distribution considered in this work, we have found it interesting to show the photograph of plasmas produced in the low-pressure environment since the plasma colors arising from the excited atoms can be visually recognized and identified with their origins as in the case of flame analysis. This would provide a useful direct visual picture of intensity distribution of each emission line, complementing the result of quantitative measurement to be presented later.

Figure 2 shows the photographs of the plasmas obtained from the black stone sample in (a) 2 Torr nitrogen gas, (b) 20 Torr helium gas, and (c) from the zircaloy plate sample in 20 Torr helium gas. It is seen that all those plasmas exhibit the typical hemispherical shape and consist of a tiny primary plasma near the sample surface surrounded by a much larger secondary plasma as commonly observed in laser-induced shock-wave plasma spectroscopy.[8,14] In Fig. 2(a), the red color mainly arises from the nitrogen emission line at 600.8 nm which lies outside the spectral window of our presented data. This was readily verified by its disappearance when the nitrogen gas was replaced by helium. It is seen from Fig. 2(b) that the plasma generated in ambient helium gas consists of two regions with distinct colors. The inner part of the plasma is dominated by magenta color associated with the calcium emission. This color is rapidly fading away at its border with the outer region which features a faint mix of orange and red colors at its rim. The plasma generated from the zircaloy sample is shown in Fig. 2(c) which exhibits layers of different colors with those of the longer wavelengths appearing farther away from the target. This interesting feature is apparently related to the many Zr emission lines corresponding to different excitation energies.[14] Since the expanding secondary plasma generated by the shock wave is undergoing decreasing temperature at its front,[8,14] a corresponding reduction in the available excitation energy is to be expected at the propagating plasma front, where the thermal excitation mostly takes place. As a consequence, emission lines originating from excited states of lower energies are expected to appear more dominantly farther away from the target surface as witnessed from the photograph. It is then important to point out here that the outermost layer in this case exhibits a dominant red color mixed with a relatively less intense of orange color, which are, respectively, related to the H I 656.2 nm and He I 587.5 nm emission. Both of them are associated with excited state of energies much higher than those related to the Zr emission lines. These observations provide useful references for the analysis of the quantitative measurement result presented later.

Figure 3 shows the emission spectra of black stone sample in (a) nitrogen gas of 2 Torr and (b) helium gas of 20 Torr, in the wavelength region from 600 to 680 nm. In Fig. 3(a), the calcium emission lines are clearly observed together with the hydrogen emission line (H I 656.2 nm). In the spectrum obtained with ambient helium gas, as shown in Fig. 3(b), the intensities of all the spectral lines are greatly enhanced along with the appearance of the He I 667.9 nm emission line, as clearly shown by the remarkable increase of H I 656.2 nm/Ca I 647.3 nm intensity ratio from 0.3 in Fig. 3(a) to 0.6 in Fig. 3(b). In addition to further confirming the expected intensity enhancement effect due to the presence of helium, this result also suggests the possible contribution of the He metastable excited state associated with the observed He emission. In other words, a part of the excited He atoms may transfer their energies and give rise to an additional excitation process for the H atoms and thereby resulting in the intensity enhancement effects. Further elaboration on this point will be given in the discussion of Fig. 5. A similar enhancement effect was also observed with zircaloy sample, although it is relatively less pronounced.

We turn next to the main focus of this experiment, namely, the measurement of time-integrated spatial distributions of the hydrogen emission intensities employing the

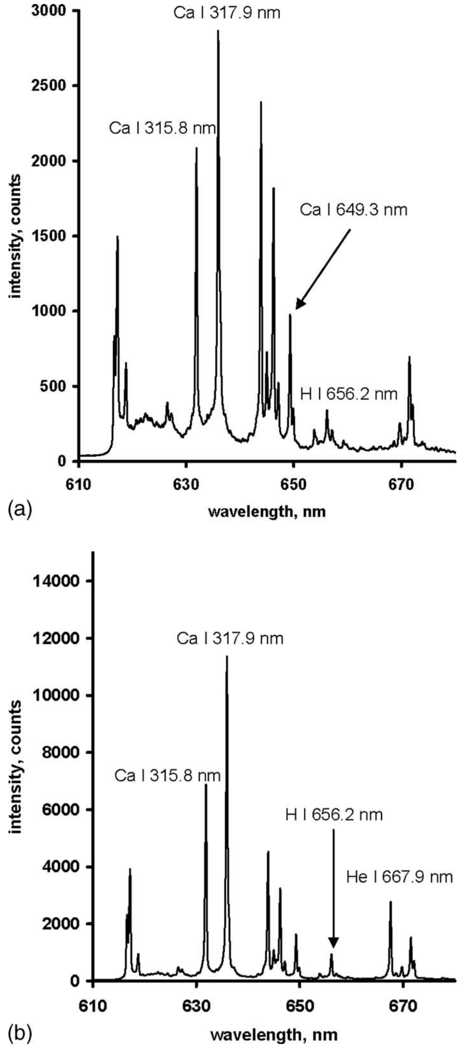

FIG. 3. The emission spectra of black stone sample in (a) 2 Torr ambient nitrogen gas and (b) 20 Torr ambient helium gas.

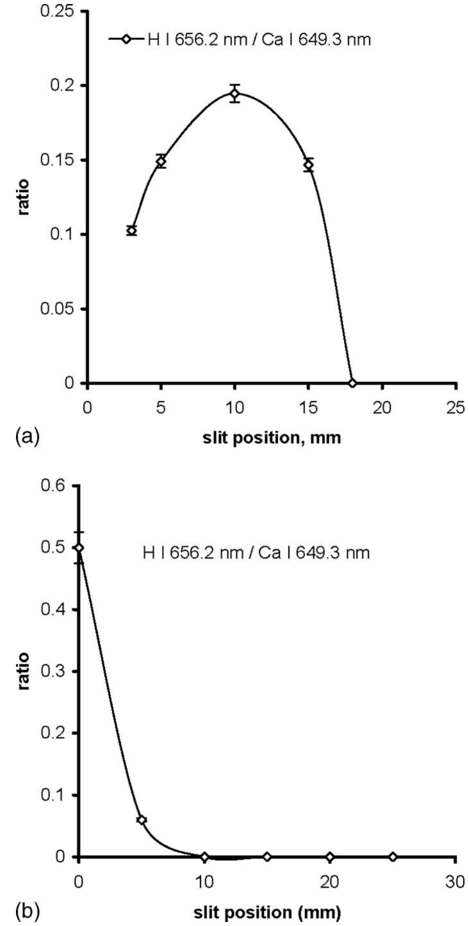

FIG. 4. Spatial distribution of hydrogen emission intensity (H I 656.2 nm) normalized by the host calcium emission intensity (Ca I 649.3 nm) for the black stone sample in (a) 2 Torr and (b) 20 Torr ambient nitrogen gases.

"plasma slicing technique" described earlier. The results are presented in Fig. 4 for the spatial distributions of hydrogen emission intensity (H I 656.2 nm) measured from the black stone sample in ambient nitrogen gas at (a) 2 Torr and (b) 20 Torr, which were normalized by the emission intensity of Ca I 649.3 nm. It is clearly seen in Fig. 4(a) that the hydrogen emission spreads out in a relatively broad but well defined area shared by the calcium emission. Meanwhile for the case of higher ambient pressure, as shown in Fig. 4(b), the hydrogen emission becomes sharply confined near the sample surface, with its measured total intensity significantly reduced from what was detected at 2 Torr. This result simply confirms the typical adverse effect of higher ambient gas pressure on the hydrogen emission intensity when shock-wave induced thermal excitation was solely responsible for the emission as reported previously in experiments with ambient gases other than helium.[14]

It is interesting to further compare this result with the spatial distribution of hydrogen emission intensity in 20 Torr ambient helium gas, as shown in Fig. 5. In this case, both the hydrogen and helium emission intensities exhibit qualitatively similar distributions featuring more diffused distributions or more extended profiles, in good agreement with the observed color distributions presented in Fig. 2, while it is in clear contrast to those found in the previous case. Additionally, both intensities appear to rise to their maxima near the far end of the plasma, where the plasma temperature is supposed to approach its minimum with correspondingly re-

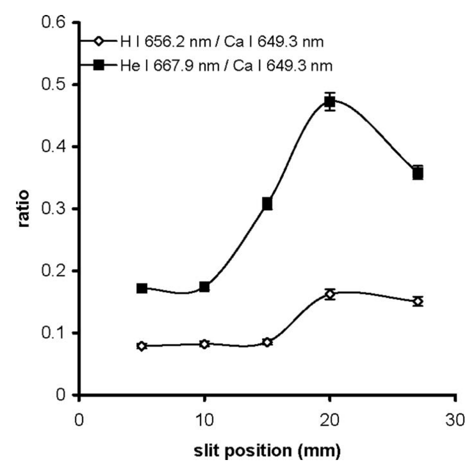

FIG. 5. Spatial distribution of hydrogen emission intensity (H I 656.2 nm) and helium emission intensity (He I 667.9 nm) normalized by the host calcium emission intensity (Ca I 649.3 nm) measured from the black stone sample in 20 Torr ambient helium gas.

duced thermal energy available for the excitation of H atoms in the plasma. It is important to recall that the excitation energies of helium and hydrogen are known to be around 23.5 and 12 eV, respectively, which are considerably higher than the 4 eV excitation energy of the calcium host element associated with its emission at 317.9 nm. This means, according to the shock-wave-induced thermal excitation mechanism, that the H and He emission intensities should be more pronounced closer to the target, with the calcium emission becoming relatively more favored farther away from the target. However, the extended curves of normalized He and H emission intensities displayed in Fig. 5, especially the rises to their maxima near the far end of the plasma clearly contradict the result expected from the excitation mechanism described above. Therefore, an additional process other than the direct thermal excitation process must be responsible for the "unexpected" observation.

It must be confessed that lacking the required comprehensive spectroscopic data for the study of this alternative excitation process, it is simply impossible to offer a detailed elucidation of its underlying physical mechanism. Nevertheless, it is worthwhile at this point to recall that the He I 667.9 nm emission is associated with one of the cascaded radiative transitions terminating at the metastable $2\,^1S_0$ excited state of He, which may provide the needed excitation energy for the delayed and persistent emission of H. Unfortunately, in view of the large energy difference between the hydrogen excited state associated with H I 656.2 nm (12 eV) emission and the $2\,^1S_0$ helium metastable excited state (20.8 eV), a direct collision-induced energy transfer involving only recoil kinetic energies of He and H is deemed highly unlikely. Instead, a more complicated process involving some as yet unproved energy transfer mechanism must be at work. One may envisage, however, that the excited He atom may release its energy through a Penning-like ionization process such as

$$\mathrm{He}^* + \mathrm{H} \rightarrow \mathrm{He} + \mathrm{H}^+ + e.$$

This is quickly followed by the recombination process leading to the neutral excited H and the subsequent radiative transition processes. This process has been considered previously in a different context, for the explanation of increasing electron density in nitrogen plasma upon He addition.[15] Admittedly, it is still difficult at this stage without indulging oneself in speculation to offer even a plausible argument for explaining the appearance of maximum emission intensities at the far end of the plasma.

Finally, it is interesting and indeed remarkable to note that when the same measurement was repeated for zircaloy sample, the same general features of H and He intensity distributions were reproduced, as shown in Fig. 6. This result clearly provides an additional support of our proposed "He-assisted excitation" hypothesis.

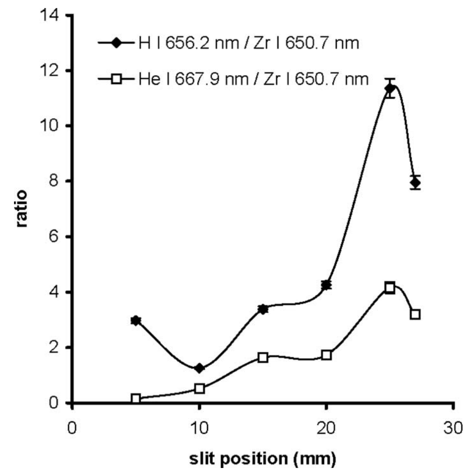

FIG. 6. Spatial distribution of hydrogen emission intensity (H I 656.2 nm) and helium emission intensity (He I 667.9 nm) normalized by host zircaloy emission intensity (Zr I 650.7 nm) measured from zircaloy sample in 20 Torr ambient helium gas.

IV. CONCLUSION

We have presented experimental evidences confirming the general improvement of spectral quality and particularly the intensity enhancement of hydrogen emission observed previously from laser-induced atmospheric-pressure helium plasma. A comparison of spatial intensity distributions of hydrogen and helium emission intensities measured from low-pressure helium plasma with that obtained from nitrogen plasma exhibits distinct unusual features unique to H emission from He plasma, indicating the unquestionable presence of an additional excitation mechanism for hydrogen other than the direct shock-wave induced thermal excitation process which is commonly known to be mainly responsible for the emission lines of heavier elements. Further analysis of the data led to the suggested "hypothesis" on the possible contribution of helium metastable excited state to the excitation of hydrogen atom giving rise to the remarkable features observed in its spatial intensity distributions. Clearly, additional experimental studies are required for the further elucidation and verification of the physical mechanism underlying the He-assisted excitation process proposed in this work.

ACKNOWLEDGMENTS

This work was partially supported through the Basic Research Grant in Physics, The Academy of Sciences for the Developing World, and Third World Academy of Sciences (TWAS) under Contract No. 06-150 RG/PHYS/AS UNESCO FR: 3240144882.

[1] R. D. Smith II, G. P. Landis, I. Maroef, D. L. Olson, and T. R. Wildeman, Weld. J. (Miami, FL, U.S.) **80**(5), 115.s (2001).
[2] A. Miziolek, V. Palleschi, and I. Schechter, *Laser-Induced Breakdown Spectroscopy (LIBS) Fundamentals and Applications* (Cambridge University Press, Cambridge, 2006).
[3] D. A. Cremers and L. J. Radziemski, *Handbook of Laser-Induced Breakdown Spectroscopy* (Wiley, Chichester, 2006).
[4] G. Asimellis, S. Hamilton, A. Giannoudakos, and M. Kompitsas, Spectrochim. Acta, Part B **60**, 1132 (2005).
[5] G. Asimellis, A. Giannoudakos, and M. Kompitsas, Anal. Bioanal. Chem. **385**, 333 (2006).
[6] G. Asimellis, A. Giannoudakos, and M. Kompitsas, Spectrochim. Acta, Part B **61**, 1270 (2006).
[7] M. Tran, Q. Sun, B. W. Smith, and J. D. Winefordner, Appl. Spectrosc. **55**, 739 (2001).
[8] K. H. Kurniawan, T. Kobayashi, and K. Kagawa, Appl. Spectrosc. **46**, 581 (1992).

[9]M. Kuzuya, H. Matsumoto, H. Takechi, and O. Mikami, Appl. Spectrosc. **47**, 1659 (1993).
[10]M. R. Joseph, N. Xu, and V. Majidi, Spectrochim. Acta, Part B **49**, 89 (1994).
[11]K. H. Kurniawan, M. Pardede, R. Hedwig, Z. S. Lie, T. J. Lie, D. P. Kurniawan, M. Ramli, K. Fukumoto, H. Niki, S. N. Abdulmadjid, T. Maruyama, N. Idris, K. Kagawa, and M. O. Tjia, Anal. Chem. **79**, 2703 (2007).
[12]M. Ramli, K. Fukumoto, H. Niki, S. N. Abdulmadjid, N. Idris, T. Maruyama, K. Kagawa, M. O. Tjia, M. Pardede, K. H. Kurniawan, R. Hedwig, Z. S. Lie, T. J. Lie, and D. P. Kurniawan, Appl. Opt. **46**, 8298 (2007).
[13]M. Ramli, K. Kagawa, S. N. Abdulmadjid, N. Idris, W. S. Budi, A. M. Marpaung, K. H. Kurniawan, T. J. Lie, M. M. Suliyanti, R. Hedwig, M. Pardede, Z. S. Lie, and M. O. Tjia, Appl. Phys. B: Lasers Opt. **86**, 729 (2007).
[14]K. H. Kurniawan and K. Kagawa, Appl. Spectrosc. Rev. **41**, 99 (2006).
[15]C. A. Henry, P. K. Diwakar, and D. W. Hahn, Spectrochim. Acta, Part B **62**, 1390 (2007).